Performance of silver nanoparticle fixed on magnetic iron nanoparticles (Fe_3O_4-Ag) in water disinfection

Roya Sharifi[1], *Amir Hessam Hassani*[1] ✉, *Homayon Ahmad Panahi*[2], *Mehdi Borghei*[3]

[1]*Department of Environmental Engineering, Science and Research Branch, Islamic Azad University, Tehran 1477893855, Iran*
[2]*Department of Chemistry, Central Tehran Branch, Islamic Azad University, Tehran 1467686831, Iran*
[3]*Department of Chemical Engineering, Sharif University of Technology, Tehran 1136511155, Iran*
✉ *E-mail: ahhassani@srbiau.ac.ir*

Published in Micro & Nano Letters; Received on 14th January 2017; Revised on 23rd August 2017; Accepted on 5th December 2017

Microbial contamination poses a serious threat to human health. The evaluation of alternative systems and their reliability for the treatment of water is essential. In this work, a new method for the deposit of more silver nanoparticles (AgNPs) on the external surface of Fe_3O_4 nanoparticles is presented. Fe_3O_4 nanoparticles were synthesised by chemical co-precipitation and were modified in two stages using 3-mercaptopropyl trimethoxysilane and grafting allyl glycidyl ether and N, N-dimethylacrylamide. Then, AgNPs were loaded onto the modified Fe_3O_4 to be used for water disinfection. The resulting nanoparticles were characterised by transmission electron microscopy, X-ray powder diffraction, Fourier transform infrared spectroscopy, vibrating sample magnetometer and thermal gravimetric analysis. Batch experiments were performed to investigate the effects of parameters such as amount of Fe_3O_4-Ag, contact time, and initial concentrations of MPN (the most probable number) and pH. The kinetic data was analysed by pseudo-first-order and pseudo-second-order equations. Results showed that the optimum conditions were a contact time of 30 min (94%), 50 mg of Fe_3O_4-Ag, and a pH was 6.5 for the maximum MPN removal efficiency (99.76%) in 750 cfu/ml MPN. On the basis of the results of fitting data, the pseudo-second-order kinetic model was selected as suitable for the data.

1. Introduction: The increase in infectious disease [1, 2] caused by contamination of water, the existence of resistant microorganisms [1] and disinfection by products in water disinfection systems have led researchers to attempt to develop new, durable and effective antibacterial materials. The application of nanotechnology can be very useful in this area and can increase the quality of life [3]. The role of silver nanoparticles (AgNPs) as a branch of nanotechnology in the treatment of water and the prevention of microbial growth [4] is greater due to their unique properties [5] as a disinfectant compared with inorganic metal oxides [6].

Recently, many studies have focused on the preparation, specification, and antimicrobial performance of nanoparticles. For example, Kim *et al.* [2] synthesised CNT-Ag (carbon nanotube-silver) and GO-Ag (grapheme oxide) nanocomposites with Ag combination proportions of 6.1 and 5.8%, respectively, and examined their inhibitory effects in samples containing *E. coli*. Zhang *et al.* [7] with the removal of limitation in the synthesis of Ag nanosheets, reported a simple, one-step, low-cost method of covering Ag nanosheets with a polymer film. Quang *et al.* [8] examined the potential to disinfect contaminated water using AgNPs embedded on silica beads at various flow rates.

Surface energy and high surface area-to-volume ratio makes the AgNPs prone to aggregation and eventually decreases their chemical and antimicrobial properties [1, 2, 6, 9]. As a perfect solution, magnetic Fe_3O_4 nanoparticles can be used to recycle [5] the residue AgNPs in water, maintain acceptable concentrations, and be cost effective. Amarjargal *et al.* [10] synthesised Ag/Fe_3O_4 nanocomposites simultaneously using the modified co-precipitation method. Yu *et al.* [11] used an efficient method to synthesise Ag–Fe_3O_4@carbon composites. Cameron *et al.* [12] investigated the impact of AgNPs on *Cryptosporidium parvum* using 500 µg/ml of AgNP. The antiparasitic effect of AgNPs was investigated against *Giardia lamblia* by Said *et al.* [13]. Su *et al.* [14] found AgNP capable of deactivating *C. parvum* more effectively than heat treatment at different temperatures. Saad *et al.* [15] used AgNP for the prevention and growth inhibition of *Entamoeba histolytica* and *C. parvum* during water treatment. Cui *et al.* [16] investigated the effects of incorporating Ag into a $\gamma-Fe_3O_4@SiO_2@TiO_2$ matrix. Zhang *et al.* [1] reported that SiO_2 played a significant role in the uniform distribution of AgNPs in the $Fe_3O_4-SiO_2$ composite. The antimicrobial effect of functionalised glass-AgNP was proven by Bharti *et al.* [17] in a batch reactor against *Pseudomonas aeruginosa, Burkholderia cepacia*, and *Acinetobacter baumannii*. Ramadan and Gijs [18] employed multiple techniques for detection of waterborne pathogens at low concentrations. Similar results were obtained by Rebecca *et al.* [19]. Xia *et al.* [6] synthesised Fe_3O_4@C@Ag nanocomposites by combining various methods to achieve higher *E. coli* removal rates compared with Fe_3O_4–AgNPs.

Many nanoparticle properties, such as size [5, 20], surface charge [5], magnetic and antimicrobial behaviour depend upon surface coat and preparation techniques. Surface modification of Fe_3O_4 by a suitable polymer as a versatile tool helps to change surface properties. Free radical polymerisation as a controlled polymerisation technique due to its distinct advantages is used to modify polymer substrate surfaces. Reactive sites on the surface must be identified before polymerisation while retaining specific bulk properties with increased biocompatibility.

The desired structure with controlled polydispersity and site-favourite functionality can be formed with grafting polymer modifications. Furthermore, the nature of interaction depends on the chemical and physical properties of the polymer. In the first step of this Letter, a Fe_3O_4 surface was modified with 3-mercaptopropyl trimethoxysilane. In the second step, modified Fe_3O_4 were grafted with N, N-dimethylacrylamide (DMAA) and allyl glycidyl ether (AGE). In the third step, Na_2S as a coupling agent was selected for the attachment of silver nanoparticles. Using this approach to achieve a material with a high capacity for the loading of more AgNPs for the removal of MPN (the most probable number) can be effective. The purpose of this article was to evaluate the possibility of applying an alternative and new material for the removal of MPN in water disinfection processes; furthermore, optimal conditions were investigated.

2. Materials and methods

2.1. Materials: Ferric chloride ($FeCl_3 \cdot 6H_2O$), ferrous chloride ($FeCl_2 \cdot 4H_2O$), silver nitrate, sodium borohydride, ammonium

doi: 10.1049/mnl.2016.0727

hydroxide (NH_4OH 25%), sodium sulphide hydrate, dioxan, and ethanol were obtained from Merck (Darmstadt, Germany). 3-mercaptopropyl trimethoxysilane, DMAA, AGE, and 2, 2′-azobis (2-methylpropionitrile) (AIBN) were purchased from Sigma-Aldrich. All chemicals were analytical graded and used without further purification.

2.2. Synthesis of magnetic nanoparticles: In this step, 2.307 g of $FeCl_3 \cdot 6H_2O$ and 3.97 g of $FeCl_2 \cdot 4H_2O$ were dissolved in deionised water (100 ml) and mixed with a magnetic stirrer. Then, ammonia solution was injected into the above mixture at 85°C, which resulted in the immediate formation of a black solution. Nitrogen gas was passed into the solution for 2 h during all stages of the reaction. At the end of 2 h, separating operations were carried out using an external magnetic field and black powder washed twice with distilled water and ethanol and allowed to dry at room temperature.

2.3. Preparation of modified Fe_3O_4nanoparticles: In the next stage, 50 ml of 5% solution (2.5 ml of 3-mercaptopropyl trimethoxysilane in 47.5 ml of dioxan) was added to Fe_3O_4 nanoparticles (3 g), and the mixture was refluxed for 3 days at 90°C. Then, the obtained magnetic precipitate was washed with dioxin (30 ml) and dried in a desiccator.

2.4. Graft polymerisation: The free radical polymerisation method was performed by adding the obtained modified Fe_3O_4 nanoparticles (3 g) to a mixture containing 10 ml of AGE, DMAA (1.5 ml), and 0.1 g of AIBN. To graft DMAA and AGE on the surface of modified Fe_3O_4 for the removal of oxygen, the mixture was injected with nitrogen. Then the degassed mixture was refluxed in an N_2 atmosphere at 65–70°C and kept in this condition for 7 h. The resultant grafted magnetic product was washed with 30 ml of ethanol to remove the adsorbed polymer and impurities and was then dried in a desiccator.

2.5. Sulphidication of grafted polymer on Fe_3O_4: Finally, a solution of 0.5 M of Na_2S (50 ml) was prepared and dispersed in 10 ml of 0.1 M buffer 5 accompanied by grafted Fe_3O_4 to make a sulphur group on the polymer chains. It was stirred under vigorous shaking (150 rpm) for 24 h at 40°C. After filtration, the obtained sample was prepared to adsorb AgNPs.

2.6. Preparation of AgNPs: To prepare the AgNPs, the method introduced by Solomon *et al.* [21] was used. After the sodium borohydride solution (2 mM, 30 ml) was prepared, it was transferred to an ice bath and placed on a magnetic stirrer. Then, silver nitrate was dropped into it. After 3 min, the reaction was complete and mixing was stopped.

2.7. Coupling of AgNPs on Fe_3O_4: To bind the AgNPs onto the appropriate site, grafted Fe_3O_4 nanoparticles were filtered after making contact with the AgNPs while being shaken at 150 rpm and room temperature. Finally, Fe_3O_4–Ag were obtained.

2.8. Characterisation: To determine the crystalline structure of the synthesised Fe_3O_4–AgNPs, X-ray powder diffraction (XRD) was recorded on a Seifert XRD 3003 PTS diffractometer (Germany) at room temperature in the range of $2\theta = 20$–80, at 40 kV and 30 mA. Transmission electron microscopy (TEM, CM 30, Philips, the Netherlands) was used to determine the size and morphology of the nanoparticles. Infrared spectra were performed on a Fourier transform infrared spectrometer (FTIR 410; Jasco, Japan) in the range of 400–4000 cm^{-1}. The thermal stability of samples was measured using thermogravimetric analysis (TGA 50-H, Shimadzu, Japan) at a heating rate of 10°C/min in temperatures ranging 30–600°C in a nitrogen atmosphere. The magnetic measurements resulting samples were examined using vibrating sample magnetometer (Meghnatis Kashan Kavir Company).

2.9. Microbial testing methods: To evaluate the performance of stabilised AgNPs on the magnetic nanoparticles, the multiple-tube method (MPN method) was used based on the standard method. To evaluate the usefulness of grafted Fe_3O_4–Ag in water disinfection, the impact of parameters such as contact time, grafted Fe_3O_4–Ag dose, MPN concentration, and pH was checked. Initially, five beakers previously sterilised by autoclaving at a temperature of 120°C for 20 min and containing 150 ml of water with the identified MPN (MPN 350 cfu/ml) was prepared, and then Fe_3O_4–Ag was added to it. Samples were shaken at 150 rpm for certain periods of time (5, 15, 30, 60, and 90 min); after separation by the magnet, the samples were added to the culture medium and incubated at 37°C for 24 h. Growth of bacteria, existence of gas, and turbidity were investigated by visual inspection. In the next stage, the optimal amount of Fe_3O_4 nanoparticles was determined by weighing Fe_3O_4–Ag (in amounts of 0.01, 0.05, 0.1, 0.15, 0.2, 0.5 and 1 g) and transferring it into the water with 130 cfu/ml MPN. Then the mixture was vortexed vigorously at 150 rpm and room temperature. To determine the effects of different concentrations of MPN on the performance of Fe_3O_4–AgNPs, MPN in amounts of 15, 30, 50, 100, 200, 500, 750, 1000, and 1500 cfu/ml was prepared and stirred for a certain time with the optimum amount of grafted Fe_3O_4–Ag. To investigate the effect of pH, after adjusting the pH values in 6.5, 7.5, and 8.5 NaOH or HCl solutions, 150 ml samples containing 15, 100, 500, and 1500 cfu/ml MPN were taken, and the optimum amount of grafted Fe_3O_4–Ag was introduced to each mixture. As in the previous stage, samples were stirred at 150 rpm and incubated for 24 h. Similar tests were done with the control group in all stages.

3. Result and discussion

3.1. Characterisation of Fe_3O_4 – Ag: The TEM image of Fe_3O_4 nanoparticles with a magnetic core for AgNPs is shown in Fig. 1. It is noted that the size distribution of the obtained sample varies from 15 to 50 nm (Fig. 1*a*), and modified Fe_3O_4 nanoparticles after grafting with DMAA and AGE maintained their spherical shape. The existence of a grey shell around the black core as an internal layer suggests that polymerisation of the modified Fe_3O_4–AgNPs was successful and resulted in the formation of an Fe_3O_4–Ag structure (Fig. 1*b*).

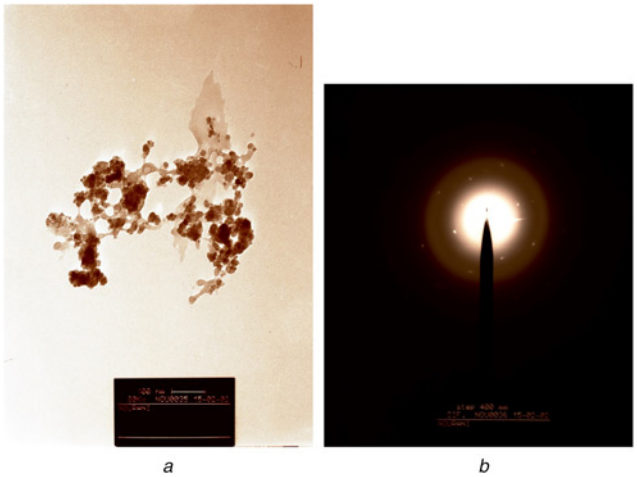

Fig. 1 *TEM image of Fe_3O_4–AgNPs*
a size distribution and
b Polymerisation of the modified Fe_3O_4–Ag

In FTIR spectra, the structure of the prepared Fe_3O_4 was revealed with a distinct peak at 589.15 cm^{-1}. The peak at 1117 cm^{-1} caused by the modification of Fe_3O_4 with 3-mercaptopropyl trimethoxysilane, which corresponds to Si–O, can be seen well in the FTIR spectrum (Fig. 2). The occurrence of a polymer group on the surface of the magnetic core was observed by bonds at about 1036 and 3693 cm^{-1} that are assigned to C–O and O–H, respectively.

The X-ray diffraction pattern was used to prove the production of AgNPs on Fe_3O_4 (Fig. 3). Characteristic peaks at 2θ of 30.078, 35.439, 43.070, 56.958, and 62.545 correspond to their indices (220), (311), (400), (333), and (440) were shown in the pattern of Fe_3O_4 NPs and are consistent with diffraction card JCPDS Card No. 01-079-0417 in position. Diffraction peaks at 2θ of 37.043, 40.308, 45.312, 64.523, and 76.09 can be indexed to (101), (102), (103), (110), and (114) planes of fcc Ag (JCPDS Card No. 01-087-0598), suggesting the existence of nanosilver on the surface of Fe_3O_4. Therefore, all data proved that Fe_3O_4–AgNPs were successfully formed.

TGA shows that Fe_3O_4 nanoparticles are stable up to 270°C (Fig. 4) and two weight losses, at 100°C and at 270–350°C, were observed. The first stage occurred because of water molecular adsorption of about 2%, and the second stage is attributed to grafting polymer decomposition on Fe_3O_4 nanoparticles which showed a weight loss of about 11%. It proves that grafting the polymers onto Fe_3O_4 nanoparticles was done successfully.

To evaluate the magnetic behaviour of nanoparticles, magnetic measurement was carried out for Fe_3O_4 and modified Fe_3O_4. Vibrating sample magnetometer measurements showed that the modified magnetic iron oxide had a smaller magnetic value and the results showed that, initially, the particles were supermagnetic. Both curves show the magnetic hysteresis (Fig. 5).

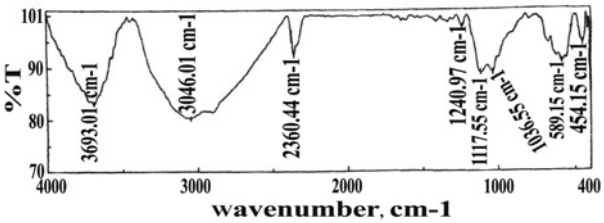

Fig. 2 *FTIR of Fe_3O_4 – Ag core–shell nanoparticle*

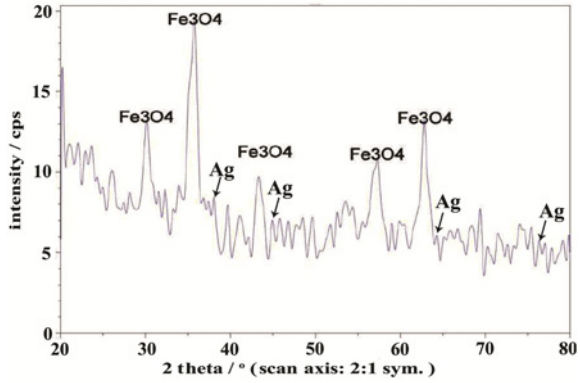

Fig. 3 *XRD patterns of Fe_3O_4–Ag nanoparticles*

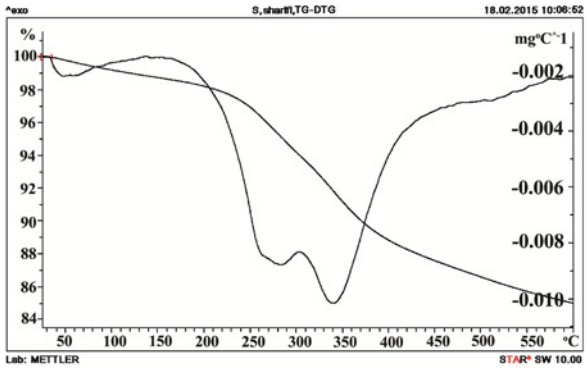

Fig. 4 *TGA images of Fe_3O_4–Ag nanoparticles*

3.2. Evaluation of the antibacterial activity of Fe_3O_4 – Ag

3.2.1. Effect of contact time: The disinfection capacity of nanoparticles was studied by experiments on such parameters as contact time, different amounts of nanoparticles, different concentrations of MPN, and different pHs, and the results are shown in Figs. 6 and 7. The effect of contact time on MPN removal percentage was examined by applying different retention times (5–90 min). The results (Fig. 6*a*) indicated that a contact time of 5 min is insufficient for the removal of MPN. The significant effect of increasing contact time on the removal of MPN can be clearly seen in the results. A high percentage of removal was achieved only after 30 min, 94% of MPN was eliminated in this time. In contact times >30 min, no significant increase in MPN removal efficiency was observed. It can be said that a good distribution of small-sized AgNPs on the surface of modified Fe_3O_4 nanoparticles prevents aggregation and results in the stability of AgNP because it is of sulphur and has a strong affinity for Ag. Consequently, it increases the antimicrobial performance of Fe_3O_4–Ag. Contact between AgNPs and bacteria causes damage and changes to their structure. The high number of sites and their being vacant at the beginning of the experiment increased the removal percentage. After during this time, due to covering of these sites no effect in removal efficiency was observed. So Fe_3O_4–AgNPs are suitable for MPN removal in water disinfection processes with a short contact time, which was determined in this study to be 30 min. The optimum contact time as determined in this study is similar to the antibacterial effect of Ag (II)O · Fe_3O_4 at 25 min for the removal of 99.99% of gram-

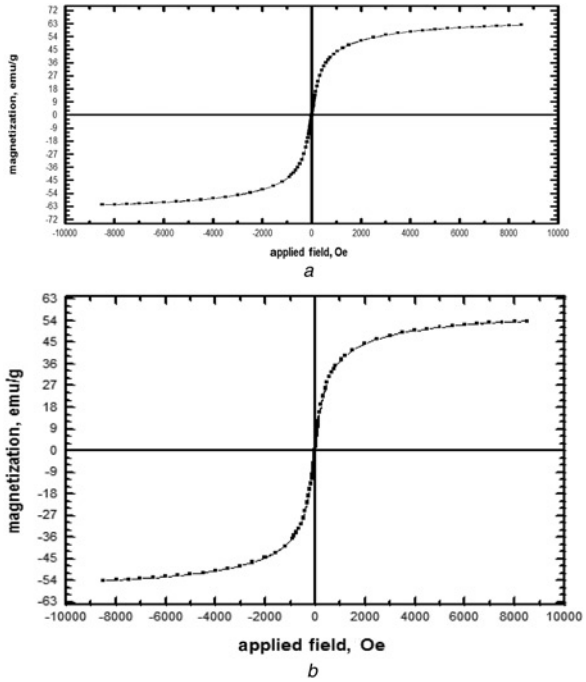

Fig. 5 *Magnetisation curves of*
a Fe_3O_4
b Fe_3O_4–Ag nanoparticles

doi: 10.1049/mnl.2016.0727

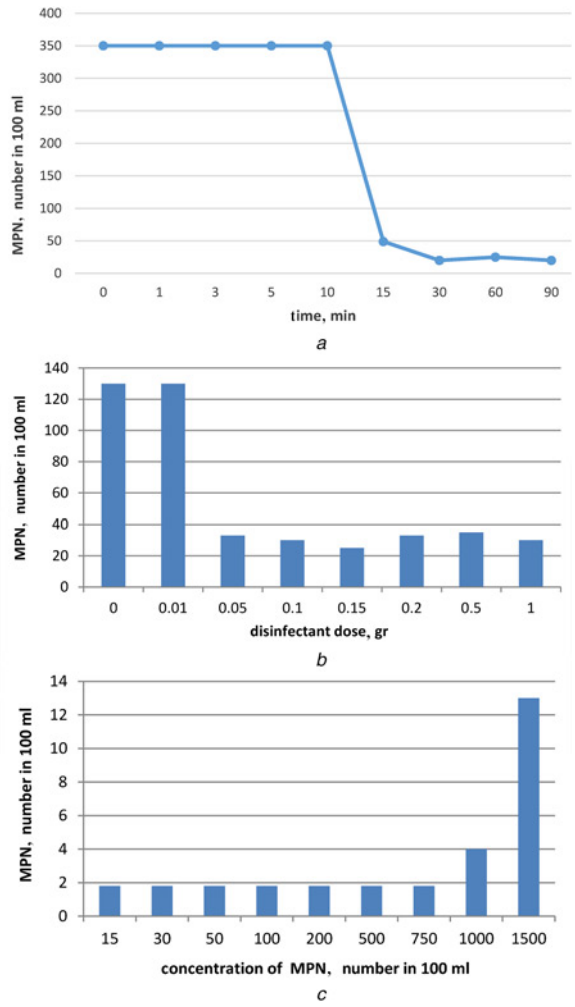

Fig. 6 *Impact of*
a Contact time
b Various amounts of nanoparticles and
c Various concentrations of MPN on Fe_3O_4–Ag nanoparticles as a disinfectant

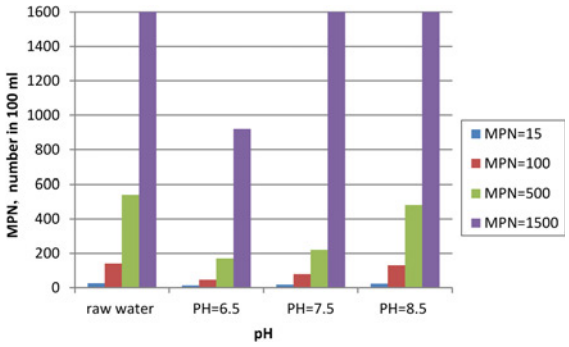

Fig. 7 *Impact of pH on Fe_3O_4–Ag nanoparticles as a disinfectant*

negative bacteria and confirms that, in this system, removal efficiency depends on contact time [15, 17, 22]. Wang *et al.* [23] indicated that *E. coli* was killed completely after 60 min of contact with Fe_3O_4@SiO_2–Ag. The results of this study showed that in the absence of SiO_2, contact time decreased to 30 min. Liang *et al.* [24] found that maximum degradation of dyes using Fe_3O_4–C–Ag was obtained after 30 min.

3.2.2. Effect of amount of Fe_3O_4 – Ag: The effects of different doses of the produced nanoparticles under the same conditions (130 cfu/ml MPN, contact time of 30 min, mixing 150 rpm and pH 8) on water disinfection were studied. The results (Fig. 6*b*) indicated that with a low amount of Fe_3O_4–AgNPs (0.01 g), the MPN of the main sample remained largely equal to that of the control group. By adding 0.05 g of Fe_3O_4 – Ag to a constant volume of water with 130 cfu/ml MPN, the removal efficiency compared to that with 0.01 g of Fe_3O_4 – Ag increased to 74.61%. This result proves that removal percentage varies based on the dose of Fe_3O_4 – Ag. Applying 0.1–0.15 g of Fe_3O_4 – Ag is more effective in MPN removal. A slight decrease in the MPN removal (~6%) was observed after using 0.5 g of Fe_3O_4 – Ag. When the dose of Fe_3O_4 – Ag in the solution was increased to 1 g, 76.41% of MPN was eliminated in 30 min. From these results, it can be concluded that low amounts of Fe_3O_4 – Ag are able to remove MPN in a short time and with an excellent performance; therefore, 0.05 g of Fe_3O_4 – Ag was selected as the optimum value. Modifying Fe_3O_4 nanoparticles with 3-mercaptopropyl trimethoxysilane helped the polymer attach to the functional group. By changing the chemical structure of the surface, synthesised nanoparticles with a high favourable surface played an important role in a greater connection of AgNPs due to the affinity for specific ligands. Thus, it enhances the ability of AgNPs to interact with pathogens by preventing their aggregation. Increasing active sites and using a high value of Fe_3O_4 – Ag resulted in greater adsorption due to the enhanced surface area. Thereby, removal efficiency was improved by increasing the possibility of a reaction between pathogens and Fe_3O_4 – Ag resulting in the creation of an electrostatic interaction. Similar types of results on surface functionalisation of Fe_3O_4 – Ag were obtained by other researcher [25, 26]. Gong *et al.* [27] revealed that Fe_3O_4 – Ag can kill different types of bacteria. Yu *et al.* [11] examined the antimicrobial activity of Ag–Fe_3O_4–C and Fe_3O_4–C at different doses. The increased mortality rate of *C. parvum* with the use of AgNP has been reported by Saad *et al.* [15].

3.2.3. Effect of initial concentrations of MPN: To achieve optimum conditions in the removal of MPN using Fe_3O_4–Ag, amounts of 15, 30, 50, 100, 200, 500, 750, 1000, and 1500 cfu/ml MPN were tested. In the optimum contact time, a significant increase in MPN removal efficiency, especially at high concentrations, was observed. Fe_3O_4 – Ag showed a removal efficiency of 88% of MPN in 15 cfu/ml MPN and in a contact time of 30 min. In 750 cfu/ml MPN, removal reached 99.76%, as shown in Fig. 6*c*. Therefore, it can be concluded that the removal of MPN depends on the initial concentration of MPN in this solution. By increasing MPN, the adsorption of MPN to the Fe_3O_4 – Ag surface is greater, and the system continues to show a greater removal rate until 750 cfu/ml MPN. Limitation of adsorption sites in the elimination of MPN for high concentration led to reducing of sites and since that sufficient amount of Fe_3O_4 – Ag in solution due to lack and saturation of this site [20] is not exist, thus removal rate decreases. Removal efficiency was reduced from 99.76 to 99.6 and 99.13% in MPN amounts of 1000 and 1500 cfu/ml, respectively. Despite this result, the MPN from 1000 and 1500 cfu/ml reached to 4 cfu/ml (99.6%) and 13 cfu/ml, which could be effective in water disinfection within 30 min. Results of previous experiments reflect the high capacity of poly(AGE/IDA-co-DMAA)-grafted silica with increasing concentrations due to the good accessibility of pb(II) to active sites [28]. The results of this experiment are compatible with the results obtained by Amarjargal *et al.* [10] regarding the use of Fe_3O_4 – Ag as a disinfectant.

3.2.4. Effect of pH: To find the effect of pH on the removal of MPN, pH values of 6.5, 7.5, and 8.5 were investigated. Since the objective was the removal of MPN and water treatment, changes to pH were applied to drinking water. The results shown in Fig. 7 demonstrated the influences of pH on MPN removal efficiency. MPN removal efficiency was reduced from 50, 67, 68.5, and

42.5% in pH 6.5 to 11.5, 7.1, 11, and 0% at pH 8.5 for 15, 100, 500, and 1500 cfu/ml MPN, respectively. Studies have indicated that in order for AgNPs to exist in a positive charge, electrostatic interaction must occur in contact with this nanoparticle and bacteria [29]. The effect of changes in pH from acidic to basic condition on the surface charge of the adsorbent can be influenced by adsorption chemistry. The extent of this change depends on the functional group of the sorbent [20]. Size [30, 31] and surface charge of AgNPs are considered important parameters, changes in these specifications can influence their antibacterial activity [29] and cause in the basic pH both the pathogen and adsorbent to be involved in a negative charge. Consequently, to electrostatic repulsion will cause removal efficiency to be reduced. Despite the influence of pH on MPN removal, $Fe_3O_4 - Ag$ has great potential in the two pHs of 6.5 and 7.5 to reduce MPN and be used in water disinfection systems. In the next section, we measured the Ag^+ release for the Fe_3O_4–Ag sample using an atomic absorption spectrophotometer at pH values of 6.5, 7.5, and 8.5. The results indicated that a decrease in pH decreased Ag^+ release at 100, 500, and 1500 cfu/ml MPN. This is consistent with the results obtained by Fauss and co-authors [30, 31]. This study also determined the effect of calcium chloride (400 mg/l) on the release of Ag ions and removal of MPN in water samples of 15 and 500 cfu/ml at pH 6.5. The results showed a low Ag ion release in the MPN solution. This could be attributed to the anionic ligands present in the $CaCl_2$ solution that led to the formation of AgCl and its precipitate in solution, reducing the removal efficiency of MPN by AgNP. The results of this experiment are compatible those obtained by Zhang *et al.* [32] that found that the stability and survival of *E. coli* by AgNP depends to divalent cation concentration and other factors.

3.3. Kinetics: To study the reaction kinetics which predict the rates of adsorption, two kinetic models were applied. Reaction kinetics at different times with 0.1 g Fe_3O_4–Ag at a pH of 6.5 and 350 cfu/ml MPN were investigated using the pseudo-first-order and pseudo-second-order equations. These two kinetic models are shown as

$$\text{Original form: } \frac{dp}{dt} = K_1(q_e - q_t) \quad (1)$$

$$\text{Linearised form: } \text{Log}(q_e - q_t) = \log q_t - \frac{K}{2.303}t \quad (2)$$

where q_e and q_t are the amounts of MPN adsorbed onto the sorbent (cfu/gr) at equilibrium and at time t, respectively, and K (min^{-1}) is defined as the equilibrium rate constant at (2). K_1 and R^2 (correlation coefficient) were calculated using the straight line plots of Log(q_e–q_e) against t.

$$\frac{dp}{dt} = k_2(q_e - q_t)^2 \quad (3)$$

Pseudo-second-order kinetics model

$$\frac{t}{q} = \frac{1}{k_2 q^2} + \frac{t}{q_t} \quad (4)$$

If the reaction kinetics of the pseudo-second order are applicable, the slope and intercept of this straight line allow k_2 and q_e to be obtained (3) and (4).

Adapting the data to the first- and pseudo-second-order kinetics determines the mechanism of adsorption [33]. By comparing the results of the first (Fig. 8) and pseudo-second order kinetics it was found that pseudo-second order kinetics represent a high correlation coefficient (0.9995) as depicted in Fig. 9. The results presented in Table 1 reveal that the experimental q value in the pseudo-second reaction kinetics was not significantly different from the predicted q value. This result indicates the suitability

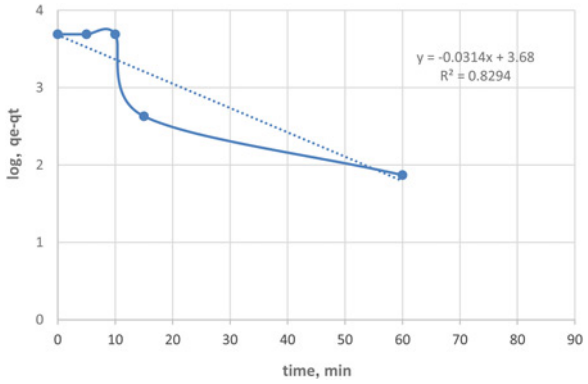

Fig. 8 *Pseudo-first–order kinetic for MPN on Fe_3O_4–Ag nanoparticles*

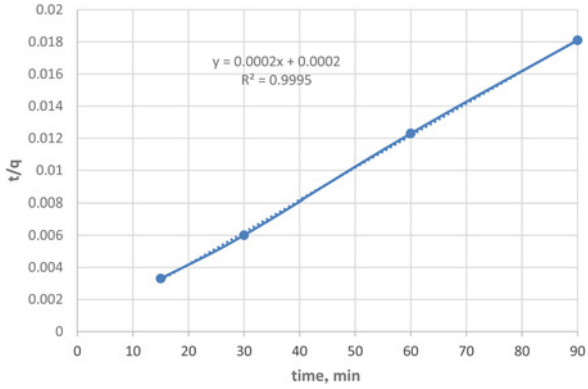

Fig. 9 *Pseudo-second-order for MPN on Fe_3O_4–Ag nanoparticles*

Table 1 Calculated parameters of pseudo-first-order and pseudo-second-order kinetics model for MPN on Fe_3O_4–Ag

Pseudo second-order	Pseudo first-order	Parameters
0.0002	0.072	K
5000	4786.30	q_e
0.9995	0.8294	R^2

and reliability of the pseudo-second-order model for reducing MPN from the samples. Tuan *et al.* [33] concluded that the adsorption kinetics with pseudo-second-order reaction was suitable for explaining the adsorption behaviour.

4. Conclusion: In this Letter, AgNPs were stabilised on magnetic Fe_3O_4 nanoparticles, and the role of functional groups in grafting DMAA and AGE by free radical polymerisation on Fe_3O_4 by 3-mercaptopropyl trimethoxysilane to better bind AgNPs onto the specified surface was investigated. After the AgNPs around branches were immobilised, the resulting modified Fe_3O_4 nanoparticles were used as a disinfectant. Research confirmed that with a small amount, this system has excellent potential for the removal of high concentrations of MPN from contaminated water in a short amount of time. The method proposed in this study prevents aggregation and oxidation by grafting Fe_3O_4 nanoparticles with the ideal group, by adding AgNPs on this affinity branche in contact with pathogens, like a bridge, it can increase removal phenomena of MPN. The separation of $Fe_3O_4 - Ag$ compared with other conventional methods due to produce pollution and significant loss after application in solution

doi: 10.1049/mnl.2016.0727

is simple. The results demonstrated that the data was better matched to the pseudo-second-order model. Although the results indicated the usefulness of magnetic nanoparticles with changes in their surface properties, some problems also exist. Removal efficiency in the water disinfection process and the quality of the residual product should be considered. Therefore, further research is necessary to investigate the safety of the produced material after the application of this novel material.

5. Acknowledgments: This work was supported by the Science and Research branch of Islamic Azad University.

6 References

[1] Zhang X., Niu H., Yan J., *ET AL.*: 'Immobilizing silver nanoparticles onto the surface of magnetic silica composite to prepare magnetic disinfectant with enhanced stability and antibacterial activity', *Colloids Surf. A, Physicochem. Eng. Asp.*, 2011, **375**, pp. 186–192

[2] Kim J.D., Yum H., Kim G.C., *ET AL.*: 'Antibacterial activity and reusability of CNT-Ag and GO-Ag nanocomposite', *Appl. Surf. Sci.*, 2013, **283**, pp. 227–233

[3] Chatterjee S., Bandyopadhyay A., Sarkar K.: 'Effect of iron oxide and gold nanoparticles on bacterial growth leading towards biological application', *J. Nanobiotechnol.*, 2011, **9**, (34), pp. 1–7

[4] Kim S.-H., Lee H.S., Ryu D.S., *ET AL.*: 'Antibacterial activity of silver – nanoparticles against *Staphylococcus aureus* and *Escherichia coli*', *J. Microbiol. Biotechnol.*, 2011, **39**, (1), pp. 77–85

[5] Kooti M., Gharineh S., Mehrkhah M., *ET AL.*: 'Preparation and antibacterial activity of Co Fe_2O_4at/SiO_2/Ag composite impregnated with streptomycin', *Chem. Eng. J.*, 2015, **259**, pp. 34–42

[6] Xia H., Cui B., Zhou J., *ET AL.*: 'Synthesis and characterization of Fe_3O_4 @ C@Ag nanocomposites and their antibacterial performance', *Appl. Surf. Sci.*, 2011, **257**, pp. 9397–9402

[7] Zhang L., Chai L., Duan J., *ET AL.*: 'One-step and cost-effective synthesis of micrometer-sized saw-like silver nanosheets by oil/water interfacial method', *Mater. Lett.*, 2011, **65**, pp. 1295–1298

[8] Quang D.V., Sarawade P.B., Jeon S.J., *ET AL.*: 'Effect water disinfection using silver nanoparticle containing silica beads', *Appl. Surf. Sci.*, 2013, **266**, pp. 280–287

[9] Kurtan U., Baykal A.: 'Fabrication and characterization of Fe_3O_4 @APTES @PAMAM–Ag highly active and recyclable magnetic nanocatalyst: catalytic reduction of 4-nitrophenol', *Mater. Res. Bull.*, 2014, **60**, pp. 79–87

[10] Amarjargal A., Tijing L.D., Im I.T., *ET AL.*: 'Simultaneous preparation of Ag/Fe_3O_4 core–shell nanocomposite with enhanced magnetic moment and strong antibacterial and catalytic properties', *Chem. Eng. J.*, 2013, **226**, pp. 243–254

[11] Yu Q., Fu A., Li H., *ET AL.*: 'Synthesis and characterization of magnetically separable Ag nanoparticles decorated mesoporous Fe_3O_4 @carbon with antibacterial and catalytic properties', *Colloids Surf. A, Physicochem. Eng. Asp.*, 2014, **457**, pp. 288–296

[12] Cameron P., Gaiser B.K., Bhandari B., *ET AL.*: 'Silver nanoparticles decrease the viability of *Cryptosporidium parvum* oocysts', *Appl. Environ. Microbiol.*, 2016, **82**, pp. 431–437

[13] Said D.E., Elsamad L.M., Gohar Y.M.: 'Validity of silver, chitosan, and curcumin nanoparticles as ani-giardia agents', *Parasitol. Res.*, 2012, **111**, pp. 545–554

[14] Su Y.H., Tsegaye M., Varhue W., *ET AL.*: 'Quantitative dielectrophoretic tracking for characterization and separation of persistent subpopulation of *Cryptosporidium parvum*', *Analyst*, 2014, **139**, pp. 66–73

[15] Saad A.H.A., Soliman M.I., Azzam A.M., *ET AL.*: 'Antiparasitic activity of silver and copper oxide nanoparticled against *Entamoeba histolytica* and *Cryptosporidium parvum* cysts', *J. Egypt. Soc. Parasitol.*, 2015, **45**, pp. 593–602

[16] Cui B., Peng H., Xia H., *ET AL.*: 'Magnetically recoverable core-shell nanocomposites γ-Fe_2O_3 @ SiO_2 @ TiO_2 –Ag with enhanced photocatalytic activity and antibacterial activity', *Sep. Purif. Technol.*, 2013, **103**, pp. 251–257

[17] Bharti S., Agnihotri S., Mukherji S., *ET AL.*: 'Effectiveness of immobilized silver nanoparticles in inactivation of pathogenic bacteria', *J. Environ. Res. Dev.*, 2015, **9**, pp. 849–856

[18] Ramadan Q., Gijs M.A.M.: 'Microfluidic application of functionalized magnetic particles for environmental analysis: focuse on waterborne pathogen detection', *Microfluid Nanofluidics*, 2012, **13**, pp. 529–542

[19] Rebecca A., Halvorson P., Vikesland J.: 'Surface-enhanced Raman spectroscopy (SERS) for environmental analyses', *Environ. Sci. Technol.*, 2010, **44**, pp. 7749–7755

[20] Attia T.M. S., Hu X.L., Qiang Y.D.: 'Synthesized magnetic nanoparticles coated zeolite for adsorption of pharmaceutical compound from aqueous using batch and colum studies', *Chemosphere*, 2013, **93**, pp. 2076–2085

[21] Solomon D.S., Bahadory M., Jeyarajasingam A.V., *ET AL.*: 'Synthesis and study of silver nanoparticles', *J. Chem. Educ.*, 2007, **84**, (2), pp. 322–325

[22] Feng L., Shen W., Feng H., *ET AL.*: 'Magnetic and sterilizing of Ag (II) O–Fe_3O_4 hybrids synthesized via mechano-chemistry', *Ceram. Int.*, 2014, **40**, pp. 6963–6972

[23] Wang X., Dai Y., Zou J.L., *ET AL.*: 'Characteristics and antibacterial activity of Ag embedded Fe_3O_4 @ SiO_2 magnetic composite as a reusable water disinfectant', *RSC Adv.*, 2013, **3**, pp. 11751–11758

[24] Liang H., Niu H., Li P., *ET AL.*: 'Multifunctional Fe_3O_4 @ C@Ag hybrid nanoparticles: aqueous solution preparation characterization and photocatalytic activity', *Mater. Res. Bull.*, 2013, **48**, pp. 2415–2419

[25] Elhouderi Z.A., Beesley D.P., Nguyen T.T., *ET AL.*: 'Synthesis, characterization and application of Fe_3O_4/Ag magnetic composites for mercury removal from water', *Mater. Res. Express*, 2016, **3**, pp. 1–9

[26] Du J., Jing C.: 'Preparation of thiol modified Fe_3O_4 @Ag magnetic SERS probe for PHA detection and identification', *Phys. Chem.*, 2011, **115**, pp. pp17829–pp17835

[27] Gong P., Li H., He X., *ET AL.*: 'Preparation and antibacterial activity of Fe_3O_4 @Ag nanoparticles', *Nanotechnology*, 2007, **18**, pp. 1–7

[28] Ahmad Panahi H., Morshedian J., Mehmandost N., *ET AL.*: 'Grafting of poly [1-(N,N-bis-carboxymethyl)amino-3-allylglycerol-co-dimethylacrylamide] copolymer onto siliceous support for preconcentration and determination of lead (II) in human plasma and environmental samples', *J. Chromatogr. A*, 2010, **1217**, pp. 5165–5172

[29] Xu H., Qu F., Xu H., *ET AL.*: 'Role of reactive oxygen species in the antibacterial mechanism of silver nanoparticles on *Escherichia coli* O157:H7', *Biometals*, 2012, **25**, pp. 45–53

[30] Jin J.C., Xu Z.Q., Dong P., *ET AL.*: 'One-step synthesis of silver nanoparticles using carbon dots as reducing and stabilizing agents and their antibacterial mechanisms', *Carbon*, 2015, **94**, pp. 129–141

[31] Fauss E.K., MacCuspie R.I., Oyanedel-Craver V., *ET AL.*: 'Disinfection action of electrostatic versus steric-stabilized silver nanoparticles on *E. coli* under different water chemistries', *Colloids Surf. B*, 2014, **113**, pp. 77–84

[32] Zhang H., Smith J.A., Oyanedel-Craver V.: 'The effect of natural water conditions on the anti-bacterial performance and stability of silver nanoparticles capped with different polymers', *Water Res.*, 2012, **46**, pp. 691–699

[33] Tuan T.Q., Son N.V., Dung H.T.K., *ET AL.*: 'Preparation and properties of silver nanoparticles loaded in activated carbon for biological and environmental applications', *J. Hazard. Mater.*, 2011, **192**, pp. 1321–1329